Design and Optimization of the Electromagnetic Actuator in Active-Passive Hybrid Vibration Isolator

Jianguo Ma[1, 2], Changgeng Shuai[1, 2], Yan Li[1, 2]

[1] Institute of Noise & Vibration, Naval University of Engineering, Wuhan, 430033, China

[2] National Key Laboratory on Ship Vibration & Noise, Wuhan, 430033, China

The design and optimization of actuators are difficult and critical for the active-passive hybrid vibration control system. In this paper, an electromagnetic actuator model is established based on Ohm's Law for magnetic circuit considering the leakage flux. The 600N electromagnetic actuators are designed and optimized based on ANSYS simulation according to the engineering request. Its transient characteristics are studied. The effects of different structural parameters on its output force are analyzed. The experimental results show that the structure parameters and output force characteristics of the designed electromagnetic actuators satisfy the practical requirement.

Keywords: Electromagnetic actuator, finite element analysis, hybrid vibration isolator, structure design.

1 Introduction

Vibration can be isolated from equipment using active or passive technology. Unlike passive vibration control, active vibration control (AVC) requires an energy feed and could respond to variations of system vibration, in which actuators play a decisive role[1-2]. Electromagnetic actuator with many advantages such as compact structure, large output force, low nonlinearity, low power consumption etc.[3] has been developed extensively. According to its working principle, the electromagnetic actuator can be classified into inertial actuator and electromagnetic (maglev) actuator. The inertial actuator which consists of a stator core with winding coil and the mass block attached to a permanent magnet is mainly used to minimize the residual force in an active vibration control system by Landau et al.[4-5]. The vibration amplitude of the clamped plate with an inertial actuator can be reduced between 6 dB and 13 dB by Paulitsch et al.[6].The inertial actuator is also applied to reduce the sound radiated by a submarine hull under propeller excitation forces by Caresta and Kessissoglou[7]. Compared with the inertial actuator, the electromagnetic actuator composed of armature, iron core, and coil produces the actuation force due to the interaction between electromagnetic fields and ferromagnetic materials. It can be widely used in the field of mechanical active control[8-11]. For example, it can be easily integrated with passive vibration isolator, in which the passive vibration isolator supports the mechanical equipment and isolates wide-band vibration and the electromagnetic actuator is used to isolate low frequency line spectrums[9,12,13]. The references 9-11 show that the hybrid vibration isolators with the electromagnetic actuator integrated into the air spring are applied in vibration isolation mounting which can be achieved a good wide-band vibration isolation and low frequency line spectrums isolation. With the increasing of the weight of isolated machines the design and optimization of active-passive hybrid vibration isolator with high load bearing capability and large output force are an important problem. The electromagnetic actuator characteristics should be improved including compact volume, low power consumption, high output force under the conditions of limited space in the air spring isolator.

In this paper, according to the working principle of electromagnetic actuator, a model of electromagnetic actuator is derived based on the Ohm's law for magnetic circuit in which the leakage flux is taken into account. The size of a 600 N electromagnetic actuator is designed and optimized. Its static and transient output force characteristics are simulated and analyzed, which is verified by the experiments.

2 Theoretical analysis of the electromagnetic actuator

Electromagnetic actuator features good force and work densities and it is convenient to be integrated into the air spring isolator. The working principle of electromagnetic actuator cannot output alternating force unless a bias force is applied on the armature in advance. Permanent magnet bias and DC current bias are the two methods to realize the bias force on the armature. The electromagnetic actuator using the DC current bias has the advantage of convenient installment. But it is need to provide extra DC bias current which not only increases the power consumption, but also causes temperature rise in the enclosed space of air spring isolator. High performance of permanent magnet is required for the actuator using the permanent magnet bias. Considering the space and power consumption limited, the permanent magnet bias is selected for the actuator. A three-dimensional geometric model as shown in Figure 1.

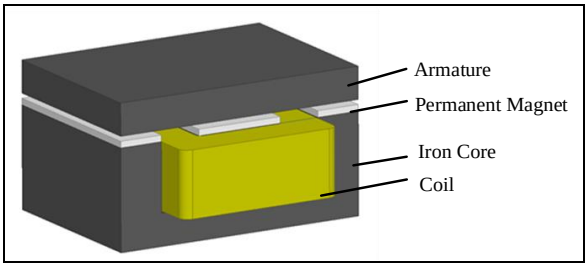

Figure 1. Three-dimensional geometric model of electromagnetic actuator.

The parameters of electromagnetic actuator include geometric parameters, performance parameters, limited parameters and object parameters. The geometric parameters mainly include that the real-time height of air gap z_t, the width of outer magnetic pole a_1, the width of the inner magnetic pole a_2, the thickness of the iron core b, the height of permanent magnet h_m, the width of coil groove in the left and right w_a, the thickness of the bottom of the iron core j, as is shown in Figure 2.

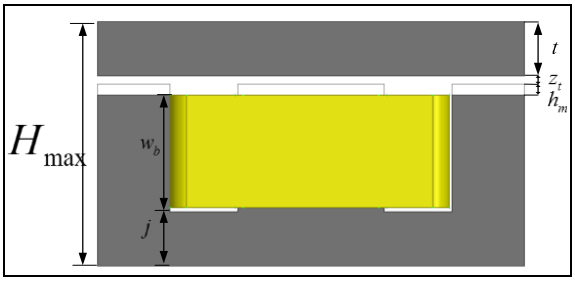

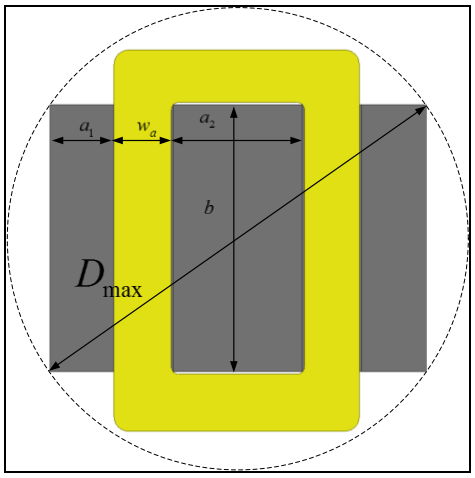

Figure 2. Dimension of E-structure actuator.

The maximum height and maximum diameter are the key parameters whether the electromagnetic actuator can be integrated into the air spring isolator. Assume the maximum is $H_{\max}$ and the maximum diameter is $D_{\max}$, which can be calculated as below:

$$H_{\max} = t + z_t + h_m + w_b + j \tag{1}$$

$$D_{\max} = \sqrt{\left(2a_1 + 2w_a + a_3\right)^2 + b^2} \tag{2}$$

The performance parameters of electromagnetic actuator include output force F_E, power consumption P, the maximum magnetic flux density B. The output force F_E is determined by the geometric parameters, the number of coil turns N and alternative current i. F_E can be shown as

$$F_E = f\left(H, D, Ni\right) \tag{3}$$

According to the references[14], the output force F_E can be also written as

$$F_E = \mu_0 \frac{a_1 a_2 b}{(2a_1 + a_2)} \frac{4H_c h_m Ni + N^2 i^2}{(z_t + \mu_0 \frac{H_c}{B_r} h_m)^2} \tag{4}$$

where the μ_0 is the air permeability, H_c is the coercive force of the permanent magnet material, B_r is the permanent remanence.

The power consumption is composed of copper loss P_{Cu} and core loss P_{Fe}. The copper loss P_{Cu} refers to the power consumption when the current flows through coil windings, which can be calculated as follow:

Assume that the thickness of the coil frame is w_c, the cross-section area of coil S_{coil} can be calculated as

$$S_{coil} = \left(w_a - w_c\right)\left(w_b - w_c\right) \tag{5}$$

Assume that the coil thankful rate is ε, the diameter d_{coil} of the coil wire can be calculated as

$$d_{coil} = 2\sqrt{\frac{\varepsilon S_{coil}}{N\pi}} \tag{6}$$

The length of coil wire l_{coil} can be calculated as

$$l_{coil} = N\left(\pi w_a + 2a_3 + 2b\right) \tag{7}$$

Assume the electrical resistivity of copper wire is ρ_{Cu}, the resistance of the coil windings can be written as

$$R_{coil} = \frac{\rho_{Cu} l_{coil}}{\pi\left(\frac{d_{coil}}{2}\right)^2} = \frac{N^2 \rho_{Cu}\left(\pi w_a + 2a_3 + 2b\right)}{\varepsilon\left(w_a - w_c\right)\left(w_b - w_c\right)} \tag{8}$$

Then the power consumption of coil windings of the electromagnetic actuator under the control current can be derived as

$$P_{Cu} = \frac{1}{2} i^2 R_{coil} = \frac{\left(Ni\right)^2 \rho_{Cu}\left(\pi w_a + 2a_3 + 2b\right)}{2\varepsilon\left(w_a - w_c\right)\left(w_b - w_c\right)} \tag{9}$$

The core loss P_{Fe} is composed of eddy-current loss P_e and hysteresis loss P_h. The eddy-current loss P_e is caused by the alternating flux in the iron core and armature. In order to reduce eddy-current loss, the iron core and armature are piled up with silicon steel sheet insulated with each other. According the numerous previous studies[15,16], the average value of P_e can be calculated as

$$P_e = \frac{\pi^2}{8\rho_s} g^2 f^2 B_{\max} V_s \tag{10}$$

In which, the ρ_s is resistivity of silicon steel sheet; the g is the thickness of silicon steel sheet; the $B_{\max}$ is the maximum magnetic flux density; the V_s is the total volume of armature and iron core.

The hysteresis loss P_h is related with the area of the magnetic hysteresis loop of silicon steel sheet, the frequency of current and the volume of actuator. Because the area of the magnetic hysteresis loop of silicon steel sheet is very small, the hysteresis loss P_h is ignored in the design process.

Hence the power consumption of electromagnetic actuator can be calculated as

$$P = P_{Cu} + P_e = \frac{\left(Ni\right)^2 \rho_{Cu}\left(\pi w_a + 2a_3 + 2b\right)}{2\varepsilon\left(w_a - w_c\right)\left(w_b - w_c\right)} + \frac{\pi^2}{8\rho_s} g^2 f^2 B_{\max} V_s \tag{11}$$

3 Design and simulation of electromagnetic actuator

3.1 Structure optimization and static magnetic characteristics simulation

How to select the appropriate design variable (DV), state variable (SV) and object function (OBJ) is very important. In the optimization of electromagnetic actuator, the DV refers to the geometric parameters that need to be optimized. Based on the analysis of the section A, the DV can be written as

$$DV = f\left(z_t, a_1, a_3, b, t, Ni, h_m, w_a, w_b, j\right) \tag{12}$$

The SV refers to the constraints in the optimization. The maximum height $H_{\max}$ and maximum diameter $D_{\max}$ are the mainly geometric constraints In order to achieve good active control effect, the output force should be large enough and the minimum output force $F_{\min}$ is the key constraint. The excessive flux density not only makes the iron core magnetic saturation which can increases the nonlinearity of the output force, but also increases the eddy current loss. Then the maximum magnetic flux density $B_{\max}$ should be limited. Hence the SV can be written as

$$V = \begin{cases} D \le D_{\max} \\ H \le H_{\max} \\ F_g \ge F_{\min} \\ B \le B_{\max} \end{cases} \tag{13}$$

When the electromagnetic actuator satisfies the DV and SV, power

consumption is set as the OBJ. Lower consumption can help to restrain temperature rise in the closed space. The object function can be defined as

$$OBJ = \min\{P_{Cu} + P_e\} \tag{14}$$

The design process of 600 N electromagnetic actuator is introduced as an example. Based on the dimension parameter of the air-spring isolator structure, the maximum height $H_{\max}$ of the designed actuator cannot exceed 120 mm, and the maximum diameter $D_{\max}$ of the designed actuator cannot exceed 190 mm. The 35WW270 steel silicon sheet is selected as the material of the iron core and armature, and its thickness g is 0.35 mm. In order to avoid the magnetic saturation, the maximum magnetic flux density cannot exceed 1.5 T. According to the demand of active control, the minimum output force cannot be less than 600N.

The steps of optimization are described as below:

(1) Firstly, obtaining the APDL optimized file which includes the information of three-dimensional model, mesh and applied load etc. through the ANSYS finite element software;

(2) Secondly, importing the APDL optimized file into the ANSYS Design Opt module and setting the DV, SV and OBJ etc.

(3) Thirdly, selecting the optimization method and running the program.

The optimized results are listed in Table 1.

Table 1. The actuator optimization parameters.

z_t (mm)	a_1 (mm)	a_3 (mm)	b (mm)	t (mm)	h_m (mm)
3	30	50	100	20	5
w_a (mm)	w_b (mm)	j (mm)	Ni	H (mm)	D (mm)
20	60	20	1200	108	181

According to the structure parameters of the optimized 600 N electromagnetic actuator, the tree-dimension model of the actuator is built by the element type of SOLID96, and the coil is modeled by the element type of SOURCE36. In order to obtain the characteristic features of the designed actuator, the theoretical and simulation calculation is carried out when the current amplitude is 6A and the results are shown as below:

The curve of output force with the changing of current is shown in Figure 3. The value of output force is larger than 600 N when the current is 6 A and the simulation results and theoretical results show agreement. The curve of maximum magnetic flux density with the changing of current is shown in

Figure 4. The values of magnetic flux density show that the magnetic flux density in the iron core and armature does not reach saturation. The distribution of magnetic flux density under different current direction is shown in Figure 5.

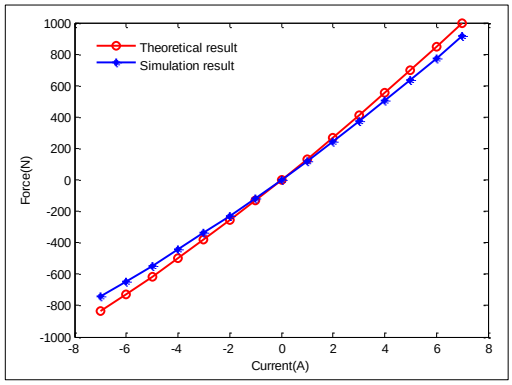

Figure 3. Output force of electromagnetic actuator.

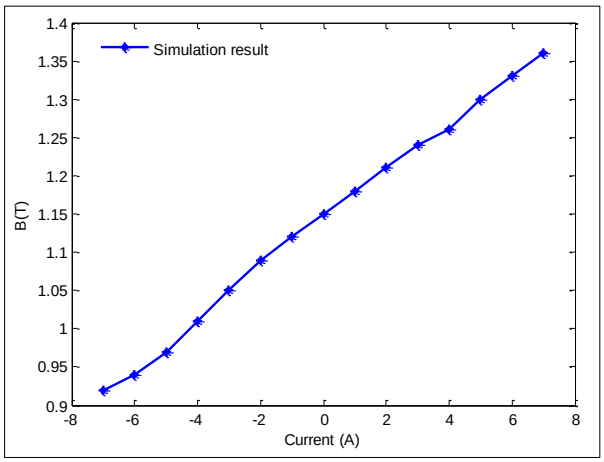

Figure 4. Magnetic flux density of electromagnetic actuator.

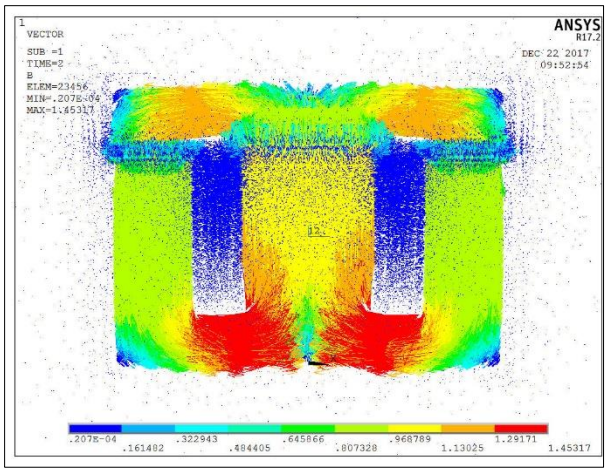

(a) with the same direction

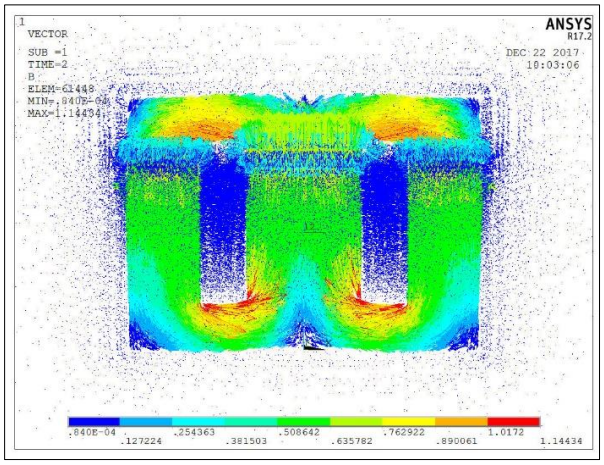

(b) with the different direction

Figure 5. Distribution of magnetic flux density of electromagnetic actuator.

3.2 Transient magnetic characteristics simulation

The characteristics of electromagnetic actuator which include transient output force, induced voltage, transient flux linkage etc. can be obtained by transient simulation analysis. In this section, transient simulation analysis of the actuator is investigated when the peak current is 6 A, frequency is 50 Hz and sampling frequency is 1000 Hz. The comparison of simulation and experimental results are shown in Figure 6 to Figure 8.

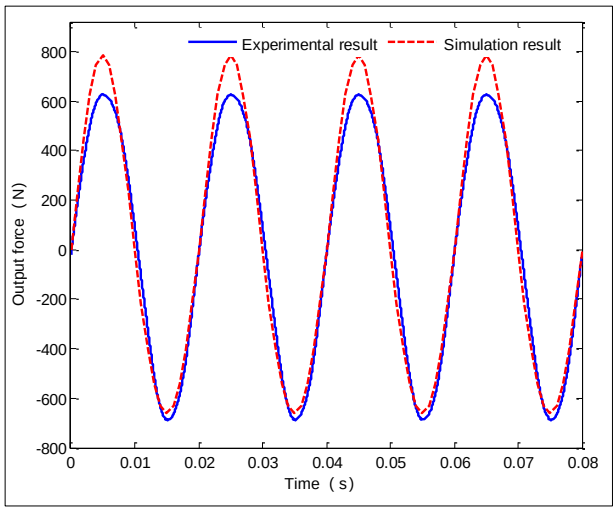

Figure 6. The comparison of simulation and experimental results for actuator output force.

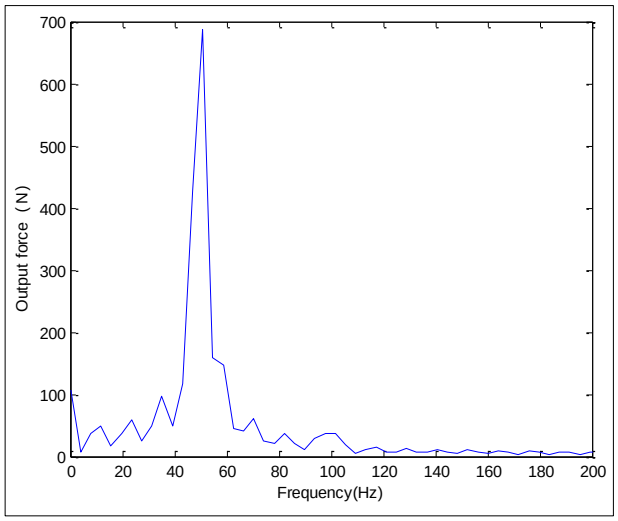

Figure 7. Spectrum of actuator simulation output force.

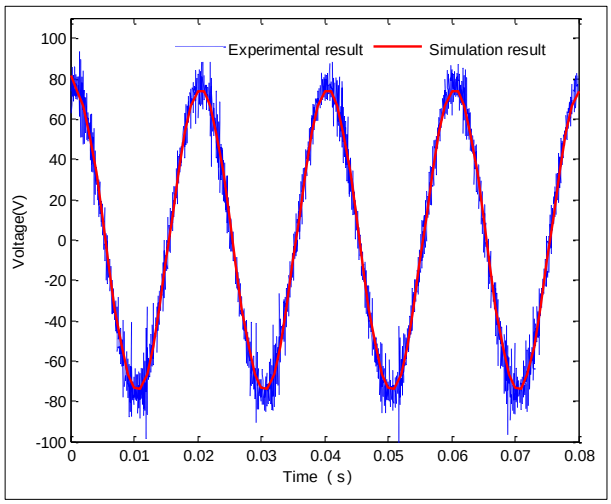

Figure 8. The comparison of simulation and experimental results for transient voltage.

The Figure 6 shows the simulation and experimental results of the output force, in which the simulation values accord with the experimental results. The spectrum of output force is shown in Figure 7 and the value of the fundamental frequency 50 Hz can be reached 687.9 N which can meet the requirements of active control. The electromagnetic actuator requires no inertial mover compared with the electromagnetic inertial-mass actuator, and it has flat amplitude-frequency and phase-frequency characteristics in the frequency range from quasi-static to several hundred Hz. The comparison of simulation and experimental voltage results is shown in Figure 8. The simulation voltage results have a good match with the experimental results, which is very important for the design of the power amplifier.

3.3 The effects of different structural parameters to the output force

According to the working principle of the electromagnetic actuator, the parameters of the permanent magnet are important for the characteristic of the actuator. The output force is simulated under different thickness permanent magnets as shown in Figure 9. With the thickness increasing of permanent magnet, the linearity of the output force increasing. However, as shown in Figure 10, with the thickness increasing of permanent magnet, the bias force is increasing. Too large bias force can weaken the stability of the hybrid isolator. Thus the permanent magnet design is important.

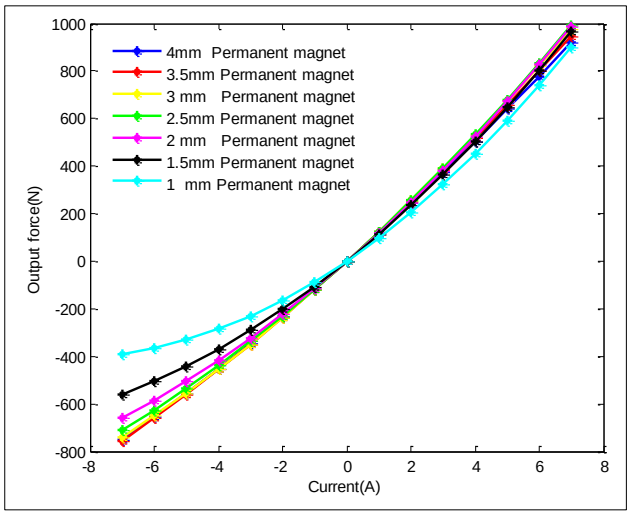

Figure 9. Output force of electromagnetic actuator with different thickness permanent magnets.

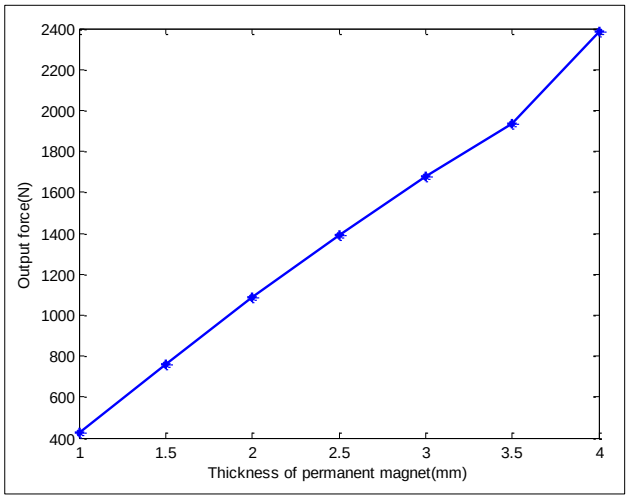

Figure 10. Bias force of electromagnetic actuator with different thickness conductive rubber.

The magnetic resistance of actuator is mainly influenced by air gap. In marine environment, air gap large enough is required to avoid crash of actuator during impact and swing, but contradictory with requirements of large output force and low power consumption. By filling magnetic conductivity rubber into air gap, the output force can be obviously improved, as shown in Figure 11, in which the output force of electromagnetic actuator is simulated under different thickness conductive rubbers. The relative permeability of conductive rubber is set 3.2 and with the thickness increasing, the output force increases. When 2.5 mm magnetic conductivity rubber is filled into the air gap, the force can be increased by 77%.

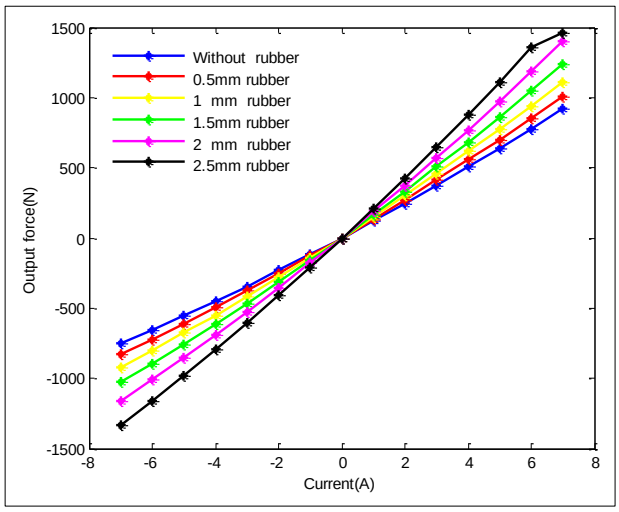

Figure 11. Output force of electromagnetic actuator with different thickness conductive rubbers.

4 Characteristic test of electromagnetic actuator

Device for testing 600 N electromagnetic actuator is shown in Figure 12, and the air gap can be regulated precisely trough MTS test machine. When the rated gap is 3 mm, the electromagnetic force is measured under different frequencies and amplitudes input current.

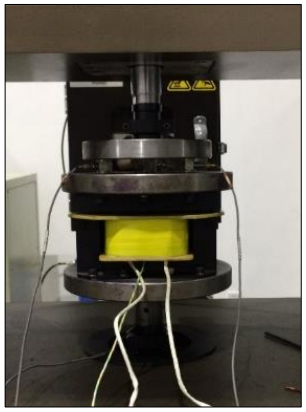

Figure 12 Magnetic flux density distribution of actuator in different time.

Figure 13 and Figure 14 show that output force is $>600N$, for different current and frequency, the amplitude gain of force/current is high and flat. Figure 15 shows that the distortion is very small, which is about 5% within 10-100 Hz. Figure 16 shows that the phase difference between force and current is very small, which is about -6.5° within 10-100 Hz, which means rapid response and good controllability. Figure 17 shows that the nonlinearity of force will increase with current increasing. But even for maximum current of 6 A, the nonlinearity of force is still smaller than 20 dB. Figure 18 shows that when actuator outputs the maximum force at 100 Hz, the maximum power consumption is only about 46 W, which is of benefit to apply in practice further.

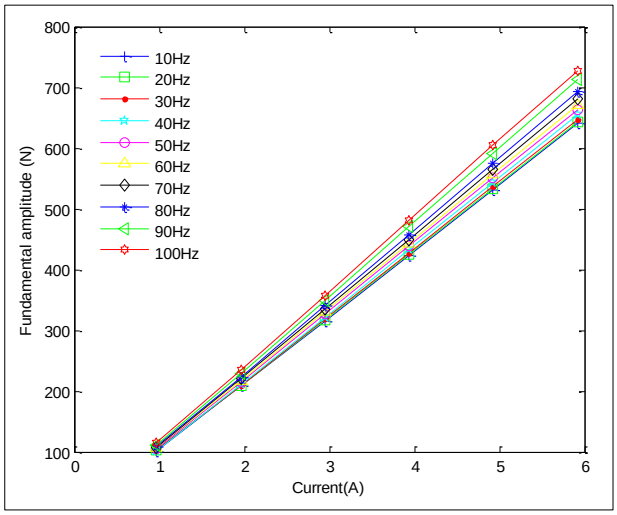

Figure 13. Output force of actuator.

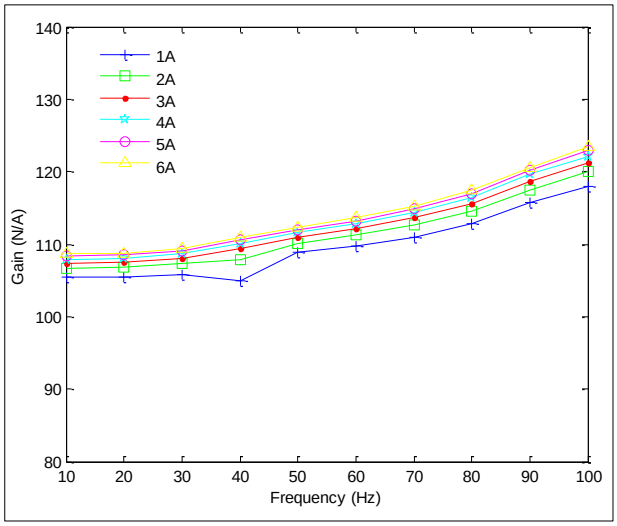

Figure 14. Gain of Force/Current.

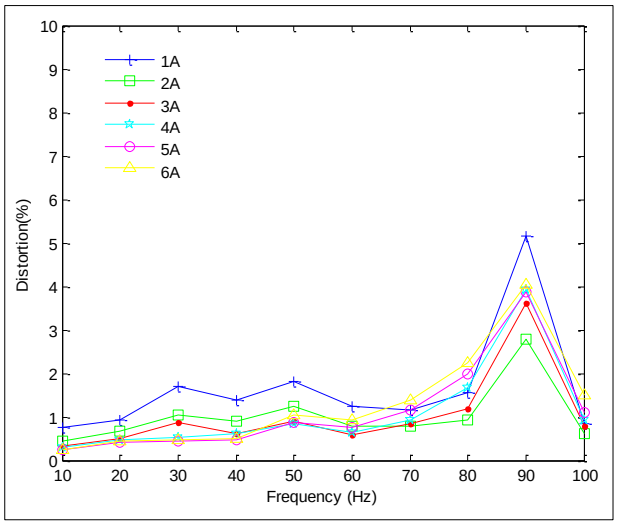

Figure 15. Distortion of force.

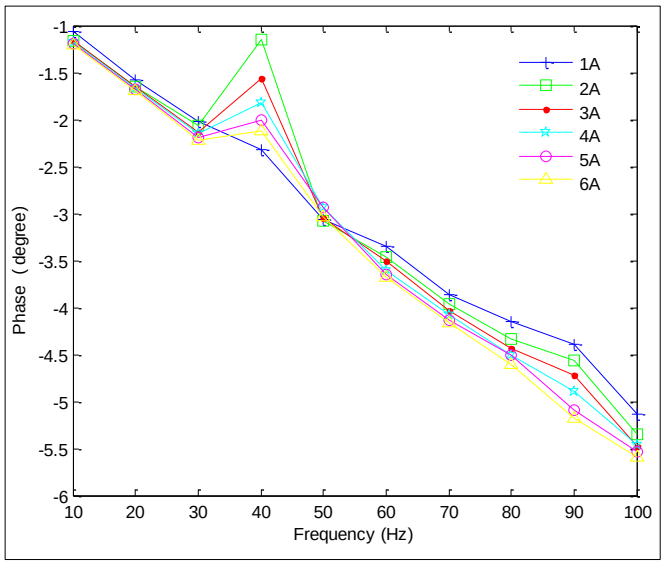

Figure 16. Phase difference between force and current.

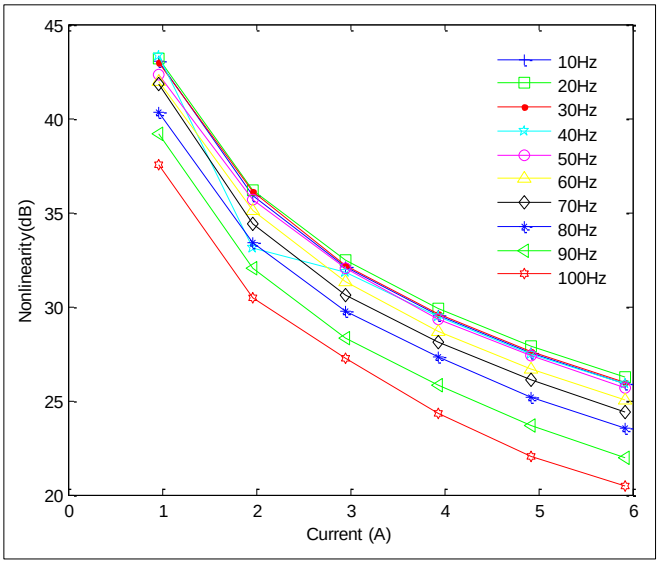

Figure 17. Energy difference between second and fundamental component of force.

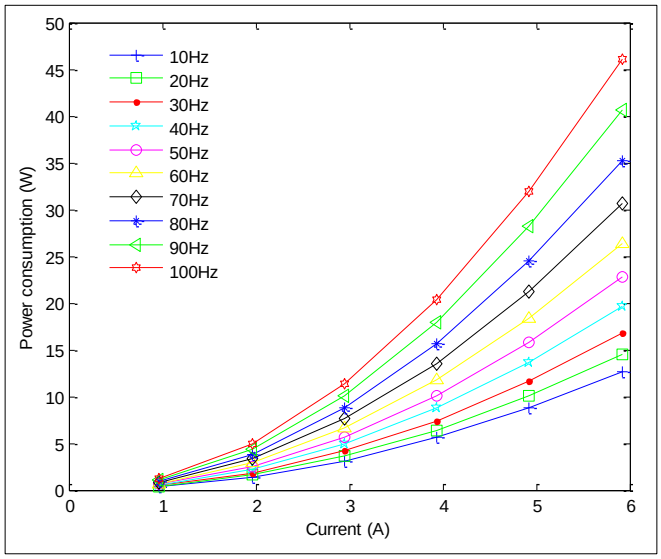

Figure 18. Power consumption of actuator.

5 Conclusions

A method of design and optimization for electromagnetic actuator in active-passive hybrid isolator is proposed. The electromagnetic actuator of permanent magnet bias is selected to use in the air-spring isolator, and theoretical model is derived. Based on the ANSYS finite element software, the structural optimization of electromagnetic actuator is simulated to obtain the actuator with high performance. Then its transient characteristics are studied. The effects of different structural parameters to its output force are analyzed. Finally, the experimental results of the designed actuator prototype show that the structure and characteristics of the actuator meet the requirements of active control.

Acknowledgement: This work is supported by the Program for New Century Excellent Talents in Universities.

References

1. Fuller, C. R., Elliott, S. J., Nelson, P. A., "Active control of vibration," London: Academic Press, pp. 59-60, 1997.
2. Elliott, S. J., "Signal processing for active control," London: Academic Press, pp. 271-319, 2001.
3. Bellmunt, O. G., Desgn, L. F., "Design rules for actuators in active mechanical system," London: Springer, pp. 5-9, 2010.
4. Airmitoaie, T. B., Landau, I. D., "Robust and adaptive active vibration control using an inertial actuator," *IEEE Transactions on Industrial Electronics*, Vol. 63, No. 10, 2016.
5. Landau, I. D., Alma, M., Martinez, J. J., Buche, G., "Adaptive suppression of multiple time-varying unknown vibrations using an inertial actuator," *IEEE Transactions on Control Systems Technology*, Vol. 19, No. 6, 2011.
6. Paulitsch, C., Gardonio, P., Elliott, S. J., "Active vibration damping using an inertial, electrodynamic actuator (DETC2005-84632)," *Journal of Vibration & Acoustics*, Vol. 129, No. 1, pp. 39-47, 2007.
7. Caresta, M., Kessissoglou, N., "Active control of sound radiated by a submarine hull in axisymmetric vibration using inertial actuators," *Journal of Vibration and Acoustics*, Vol. 81, No. 134, pp. 1-8, 2012.
8. Nitu, C., Gramescu, B., Nitu, S., "Application of electromagnetic actuators to a variable distribution system for automobile engines," *Journal of Materials Processing Technology*, Vol. 161, No. 2005, pp. 253-257, 2004.
9. Li, Y., He, L., Shuai, C. G., Wang, C. Y., "Improved hybrid isolator with maglev actuator integrated in air spring for active-passive isolation of ship machinery," *Journal of Sound and Vibration*, Vol. 407, No. 2017, pp. 226-239, 2017.
10. Li, Y., He, L., Shuai, C. G., Wang, F., "Time-domain filtered-x-Newton narrowband algorithms for active isolation of frequency-fluctuating vibration," *Journal of Sound and Vibration*, Vol. 367, No. 2016, pp. 1-21, January 2016.
11. Wang, C. Y., He, L., Li, Y., Shuai, C. G., "A multi-reference filtered-x-Newton narrowband algorithm for active isolation of vibration and experimental investigations," *Mechanical Systems and Signal Processing*, Vol. 98, No. 2018, pp. 108-123, 2017.
12. Shin, Y. H., Moon, S. J., Kim, J. M., Cho, H. Y., "Design considerations of linear electromagnetic actuator for hybrid-type active mount damper," *IEEE Transactions on Magnetics*, Vol. 49, No. 7, 2013.
13. Kitayama, F., Hirata, K., Sakai, M., "Proposal of a Two movers linear oscillatory actuator for active control engine mounts." *IEEE Transactions on* Magnetics, Vol. 49, No. 5, May 2013.

14. Ma, J. G., Shuai, C. G., Li, Y., "Experimental study on the electromagnetic actuator-air spring vibration isolator," 24th International Congress on Sound and Vibration, London UK, 2017.
15. Barbisio, E., Fiorillo, F., Ragusa, C. S., "Prediction loss in magnetic steels under arbitrary induction waveform and with minor hysteresis loops" *IEEE Transactions on Magnetics*, Vol. 40, No. 4, pp. 1810-1819, 2004.
16. Bertotti, G., "General properties of power losses in soft Ferromagnetic materials," *IEEE Transactions on Magnetics*, Vol. 24, no. 1, pp. 621-630, 1988.

The author can be reached at: mjianguo0722@163.com.